

Dong Woo Jung
Young Jun Kim
Young Jun Yang
Sun Hong Kwon

<https://doi.org/10.21278/TOF.43106>
ISSN 1333-1124
eISSN 1849-1391

WAVE RUN-UP PHENOMENON ON OFFSHORE PLATFORMS: PART 1. TENSION LEG PLATFORM

Summary

This study reports on an extensive experimental campaign carried out to evaluate non-linear waves applied to offshore structures in extreme marine environments. An offshore tension leg platform (TLP) model was used to observe the waves around a fixed-type offshore structure. The wave amplitude measured in the experiments of this study was indicated as a wave run-up ratio. Both the first-order analysis and the analysis of the entire wave amplitude were described. The experimental results were compared with the calculations from a potential-based code in order to verify the effectiveness of the developed technology.

Key words: wave run-up; order analysis; tension leg platform; wave basin

1. Introduction

Many offshore platforms are operated for extracting natural resources and executing marine operations. The conditions of extreme natural environments must be considered in order to safely operate offshore structures, although some uncertainty may exist due to unexpected events. The wave run-up is one of the phenomena which may lead to unexpected events. The wave run-up is defined as the wave elevation close to the floating structure disturbed by the floating structure (Figure 1). In terms of design, accurate estimation of the positive wave run-up and deck impact has been considered challenging, especially for column-based platforms such as semi-submersibles and tension leg platforms. However, typical potential-flow based solutions cannot precisely estimate the complicated, non-linear flow around a column-based platform.

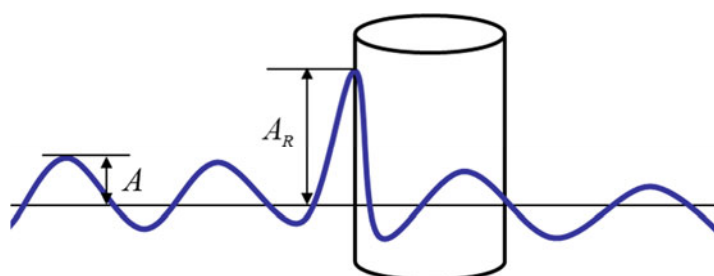


Fig. 1 Description of wave run-up

Several studies on the wave run-up around offshore structures have been performed. Eatock-Taylor and Sincock (1989) proposed the use of a free surface amplitude near a tension leg platform (TLP) during regular waves as a contour plot by using a hybrid element technique. Niedzwecki and Huston (1992) compared each wave run-up according to the distance between the columns of a TLP model and the existence of a pontoon in the experiment and concluded that there exists a connection between wave run-up and columns. Stansberg et al. (2005) performed empirical and theoretical analyses on different types of column-based platforms; they also proposed an algorithm for calculating wave-in-deck impact loads by taking Kaplan's approach. Ramirez et al. (2013) performed an experiment on the wave run-up generated loads on a slender circular cylinder and claimed that extreme run-up events occurred in the case of breaking and nearly breaking waves. Abdussameia et al. (2016) performed an experiment on a rigid TLP model under extreme wave event and measured the impact load on the deck with different deck clearance. Nam et al. (2013) developed a non-linear wave run-up analysis method that conducts a Cartesian-grid-based flow simulation on a semi-submersible platform with two columns and compared the wave run-up of the simulation with the experiment; they also showed that a non-linear nearly trapped mode exists between the columns. Matsumoto et al. (2013) compared wave elevation near a large semi-submersible unit calculated by linear and non-linear solvers. The authors concluded that consideration of the non-linear effect clearly improved the accuracy of the prediction of wave elevation.

Thanks to the rapid development and easier application of a computational fluid dynamics (CFD) solver, various papers deal with the fluid-structure interaction. Iwanowski et al. (2009) carried out a simulation on a fixed semi-submersible shape model. Also, various results on the wave run-up of a vertical circular cylinder can be found in many papers, eg. in Cao et al. (2011) and Chen et al. (2014).

A previous study by Han et al. (2014) observed the wave run-up near a truncated cylinder under regular wave conditions. Moreover, an experiment was performed on a single cylinder and a double-array cylinder with various gaps. In these experiments, different periods and wave steepnesses were combined to examine diffraction waves caused by the columns. A fixed-type offshore structure with the shape of a simplified pontoon was used as an experimental model. To emphasize the effects of the columns and the pontoon on the wave run-up, appendages of the TLP model were not considered.

In this paper, the wave run-up on fixed column-based offshore structures is measured under different wave steepness conditions to analyse non-linear phenomena on the column-based floating offshore structures operating in extreme marine environments. A fixed-type offshore structure with the shape of a simplified pontoon was used as an experimental model. To emphasize the effects of the columns and the pontoon on the wave run-up, appendages of the TLP model were not considered. In total, eight wave probes were installed and an order analysis was performed, and the first harmonic waves were compared with a commercial potential-flow solver (HydroStar, Bureau Veritas) to verify the validity of the experiment. Finally, the first-order waves were compared with the total non-linear waves to monitor the non-linear phenomena on each wave probe.

2. Materials and Methods

2.1 Experimental setup

The experimental model was an offshore TLP model at a scale of 1:100. This TLP model structure consisted of four rounded columns and a ring-type pontoon with a curved bottom. The dimension of each part the model is illustrated in Figure 2.

The experiment was performed in a 3D towing tank of a size of 100 m × 8 m (W) × 3.5 m at the National Fisheries Research and Development Institute (NFRDI). Eight wave probes were installed in the model. Two wave probes were installed 4.5 m from the centre of the model in the direction of the wavemaker and 4 m on the right-hand side of the centre of the model in the direction of the incident wave. The schematic view and detailed locations of the wave probes are indicated in Figures 3 and 4 and Table 2. The model was located 23.5 m from the wavemaker, and the distance between the model and the wave absorber was 61.5 m.

Since the objective of the study was to observe the wave run-up on the fixed-type offshore platform, the TLP model was assumed to be fixed and no motion was allowed. Figure 5 shows the experimental setup.

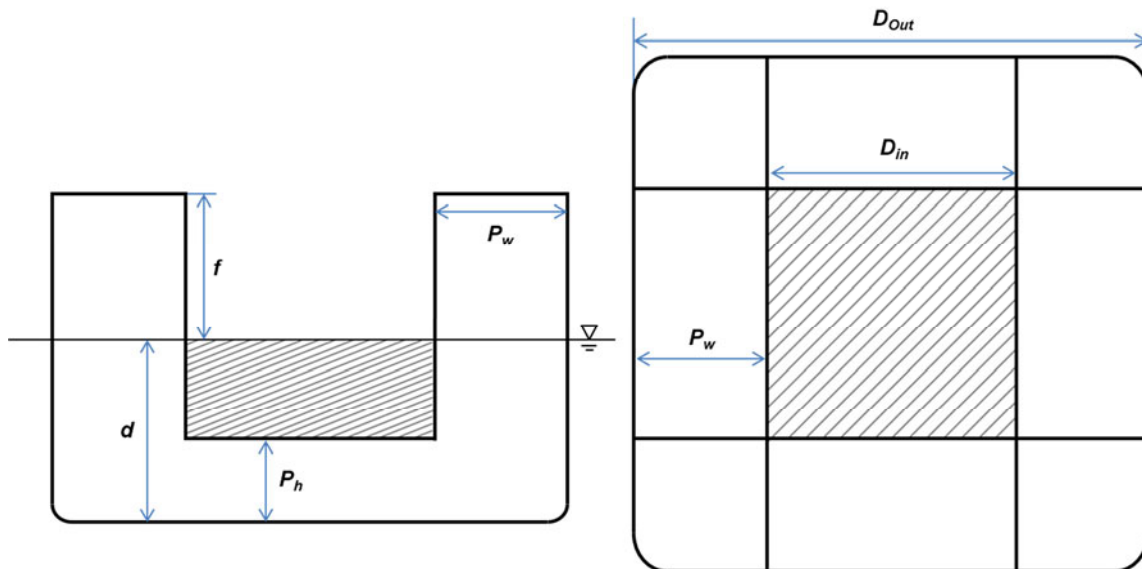


Fig. 2 Dimensions of the experimental model

Table 1 Dimensions of the experimental model

| Dimensions | Model scale (1:100) |
|--------------------------------------|----------------------------------|
| D_{out} (distance outside columns) | 1.103 m |
| D_{in} (distance inside columns) | 0.570 m |
| P_w (pontoon width) | 0.2665 m |
| P_h (pontoon height) | 0.11875 m |
| d (draft) | 0.260 m |
| f (freeboard) | 0.220 m |
| Material | Fiber Reinforced Plastic (F.R.P) |

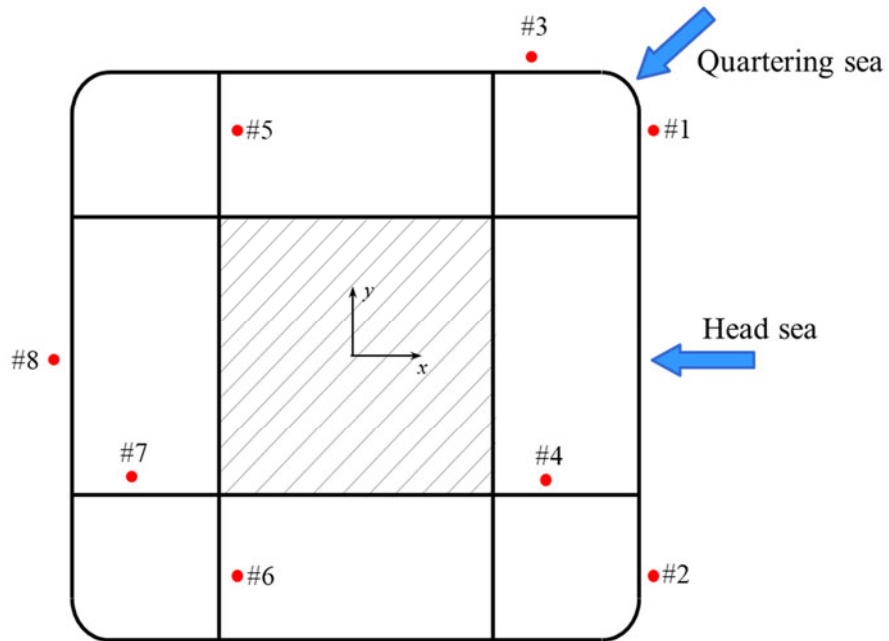


Fig. 3 Positions of wave probes

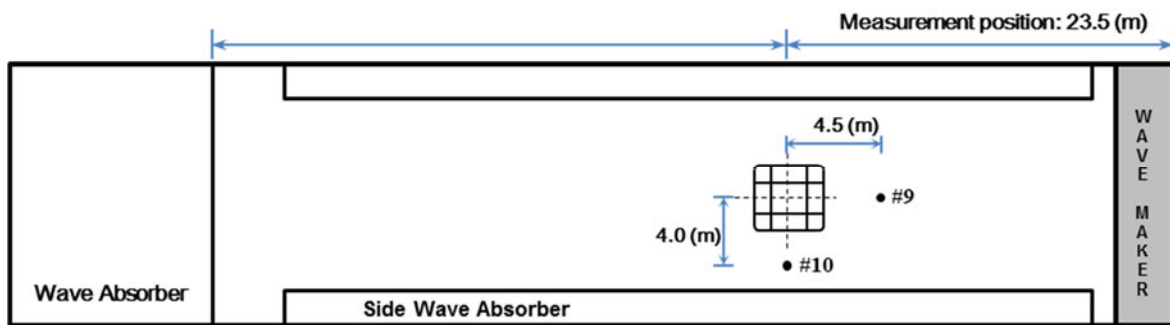


Fig. 4 3D towing tank and positions of incident wave probes

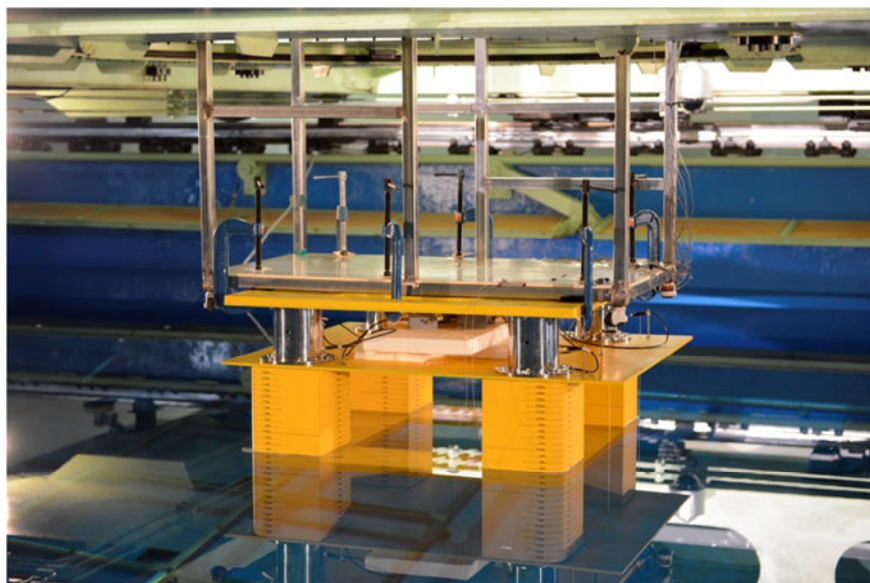


Fig. 5 Setup of the experimental model

Table 2 Positions of wave probes

| Wave probe number | Wave probe position | |
|------------------------|---------------------|---------|
| | x (m) | y (m) |
| Wave probe #1 (Capa.) | 0.5665 | 0.4700 |
| Wave probe #2 (Capa.) | 0.5665 | -0.4700 |
| Wave probe #3 (Capa.) | 0.3665 | 0.5665 |
| Wave probe #4 (Capa.) | 0.4000 | -0.2700 |
| Wave probe #5 (Capa.) | -0.2700 | 0.4700 |
| Wave probe #6 (Capa.) | -0.2700 | -0.4700 |
| Wave probe #7 (Capa.) | -0.4000 | -0.2700 |
| Wave probe #8 (Capa.) | -0.5665 | 0 |
| Wave probe #9 (Resi.) | 4.500 | 0 |
| Wave probe #10 (Resi.) | 0 | 4.000 |

2.2 Test conditions

To observe the wave run-up near the structure affected by regular waves, an experiment was performed using six periods between 7 sec and 15 sec under the conditions of head sea (180°) and quartering sea (225°). Moreover, the wave steepness was adjusted based on the wave height-to-wave length H/λ ratios of 1/50, 1/30, 1/16, and 1/10 to examine the wave run-up according to the changes in the wave steepness. This experiment was performed on 48 cases, and the test conditions and incident wave amplitudes are indicated in a real scale in Table 3. Two wave amplitudes are given in the table. The first one is the wave amplitude calculated from wave steepness and dispersion relation. The value in brackets is the wave amplitude measured during the wave calibration procedure before the model was established. The difference between the two values is within 5 percent, except in the case ‘T15 Steepness 1/10’, due to the limit of the wavemaker. However, the difference between the two values is not an important issue, since ‘wave steepness’ is introduced only to show the non-linearity of the wave, and every result reported in the paper is non-dimensionalized with respect to the measured wave amplitude.

Table 3 Test conditions and incident wave amplitude

| Wave heading: 180°, 225° | | Wave period, T(sec) | | | | | |
|-----------------------------|------|---------------------|------------------|------------------|------------------|--------------------|--------------------|
| Incident wave amplitude (m) | | 7 | 8 | 9 | 10 | 12 | 15 |
| Wave steepness | 1/50 | 0.765 (0.740) | 1.000 (0.976) | 1.265 (1.278) | 1.561 (1.488) | 2.248 (2.254) | 3.513 (3.502) |
| | 1/30 | 1.275 (1.279) | 1.665 (1.607) | 2.108 (2.137) | 2.260 (2.547) | 3.747 (3.811) | 5.855 (6.028) |
| | 1/16 | 2.391 (2.367) | 3.123 (3.104) | 3.952 (3.937) | 4.879 (4.834) | 7.026 (7.123) | 10.978 (10.995) |
| | 1/10 | 3.825 (3.963) | 4.996 (4.825) | 6.323 (6.142) | 7.806 (7.546) | 11.241 (10.997) | 17.565 (16.623) |

2.3 Wave data analysis

As can be seen in Table 2, ten wave probes were installed in the wave basin. The sampling frequency of every wave probe was 100 (Hz). All signals were low pass filtered and used to delete the electric noise from the measuring devices.

Since the incident wave was harmonic, the resulting wave amplitudes measured on the wave probes should have been harmonic. However, for some test cases, the incident wave was very high and the results from wave probes were highly non-linear. Figure 6 shows the general wave profile obtained from the wave probes. Only several wave periods, when the wave was fully developed but there was no reflection wave, were selected to calculate the averaged wave amplitude. The number of selected waves was different in every case due to the speed of the reflection wave; however, at least five wave periods were considered for every case.

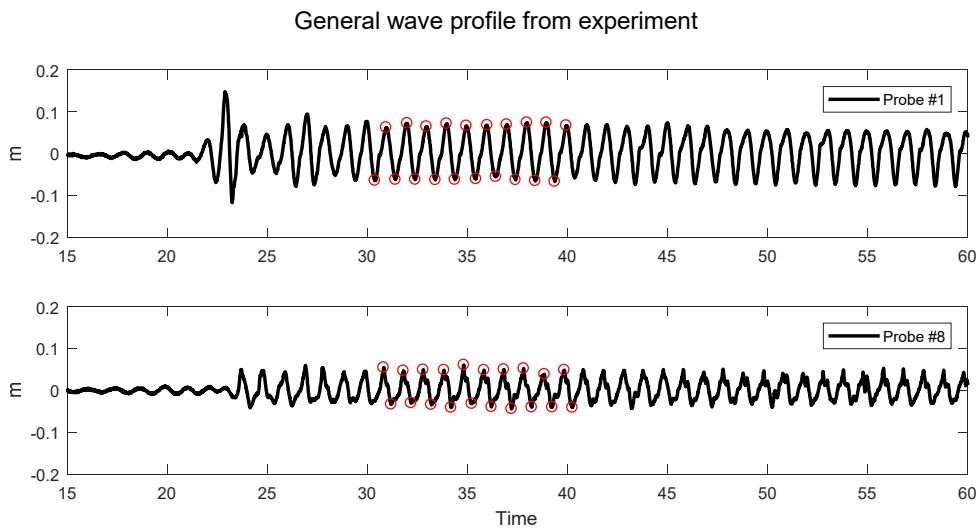


Fig. 6 Typical time series of waves

2.4 Numerical simulation setup

The wave amplitude at the wave probe was calculated by using HydroStar (V.6.3) to validate the experimental result. HydroStar is a linear potential flow solver based on the Boundary Element Method (BEM). The details on the integral equation and the related green function are described in detail by X. B. Chen (2004).

Quadrilateral panels were used as grids of this model, and a total of 11,840 panels were considered. When the linear boundary element method is used in the naval application, 11,840 panels of mesh are known to be sufficient. The hydrodynamic meshes used to perform HydroStar calculations are presented in Figure 7.

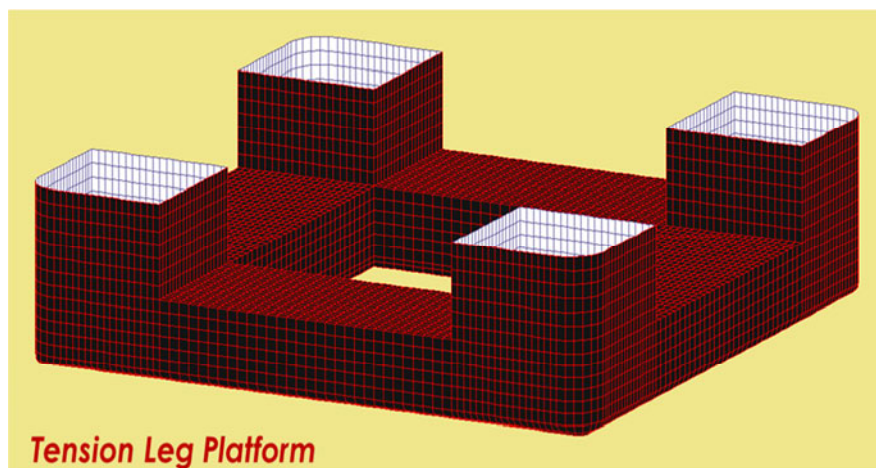


Fig. 7 Numerical hydrodynamic mesh

3. Results

3.1 Wave elevation and wave run-up

The wave amplitude measured before the model was set up was defined as the incident wave amplitude A . On the other hand, the diffracted wave amplitude measured after the installation of the model was defined as the wave run-up A_R . To compare the wave amplitude with 4 different steepnesses, the wave amplitude is non-dimensional with respect to the incident wave amplitude. This is called the ‘wave run-up ratio’ and defined as:

$$\text{Run up ratio} = \frac{A_R}{A}. \quad (1)$$

Two different filters were applied to the wave run-up. One was the band pass filter, which considered only the first harmonic amplitude and was used to compare the result with the linear potential solver. Another filter was the low pass filter, which removed only the electric noise and was used to observe the realistic non-linear wave run-up. Therefore, all results were separated into ‘the first order analysis (band pass filter)’ and ‘the full analysis (low pass filter)’. The ‘first order analysis’ compared mainly the wave run-up with the potential solver to verify the experimental result. On the other hand, the ‘full analysis’ focused on its non-linear property.

3.2 Wave run-up – Head sea (180°)

Figures 10-1 and 10-2 show ‘the first order analysis’ wave run-up ratios in the head sea condition. On the other hand, Figures 11-1 and 11-2 show ‘the full analysis’ which used a low pass filter only. The black solid line indicates the wave run-up ratio from the linear potential solver which was used to verify the experimental result. Other solid lines indicate the wave run-up ratios according to the wave steepness.

In Figures 10-1 and 10-2, the symmetry between Probe#1 and Probe#2 and the symmetry between Probe#5 and Probe#6 gives the verification of the experimental setup. As a result, these wave probes have a symmetry result, except for the case with the wave steepness of 1/10. For the wave probes located at the bow and outside of the model, such as Probe#1, Probe#2, and Probe#3, the wave run-up ratios from the experiment and HydroStar were similar regardless of the wave steepness. However, the experiment gives lower wave run-up compared to HydroStar at the location where the wave escapes, such as Probe#7 and Probe#8. Especially in the case of a period longer than 9 seconds, the difference between each wave steepness was large and the run-up ratio decreased as the wave steepness increased.

In Figures 11-1 and 11-2, wave probes Probe#1, Probe#2, Probe#5 and Probe#6 still have the symmetric property with a non-linear wave. The most significant wave run-up was observed at Probe#5 and Probe#6. The wave run-up at Probe#5 and Probe#6 reached about three times the incident wave amplitude over a period of 9 sec. Such amplification is supposed to be a non-linear phenomenon that occurs due to the pontoon and the nearly trapped mode generated between the front column and the rear column. The nearly trapped mode became more noticeable as the wave steepness increased. The non-linear phenomenon where the wave run-up ratio was amplified was also observed at the point where the wave first reached the model in the period of 7 sec, as shown at Probe#1 and Probe#2. In the cases of Probe#7 and Probe#8, the wave run-up ratio gives significantly higher results than the first-order analysis due to the non-linear components.

Except for Probe#3 only, there is a noticeable change in the wave run-up ratio along with the increase in the wave steepness. However, Probe#3 gives almost the same run-up ratio regardless of the wave steepness. Since Probe#3 is positioned outside of the model, it might be possible to assume that the amplification and the reduction of the wave run-up ratio along with the change in the wave steepness occurs from the internal wave inside the model because of the columns and pontoons.

3.3 Wave run-up – Quartering sea (225°)

Like in the previous chapter, Figures 12-1 and 12-2 present the ‘first order analysis’ wave run-up ratios in the quartering sea condition and Figures 13-1 and 13-2 present the ‘full analysis’.

In Figures 12-1 and 12-2, the symmetry between Probe#1 and Probe#3, the symmetry between Probe#4 and Probe#5 and the symmetry between Probe#6 and Probe#7 can be compared to verify the experimental result, though the wave probes are not positioned exactly at the symmetry point. As a result, it is possible to find the symmetry of the mentioned wave probes. The wave run-up ratio from the wave probes located at the bow of the model such as Probe#1 and Probe#3, have a result closer to the result obtained from the linear potential solver. In contrast, the wave probes located at the points from which waves escape, such as Probe#6, Probe#7, and Probe#8, have lower wave run-up ratios in the experiment, especially in the case of very long waves ($T > 12$ sec). For Probe#4, Probe#5, Probe#6, and Probe#7, the HydroStar results showed that a resonance peak occurred. Moreover, those resonance peaks were measured in the experiment at Probe#6 and Probe#7.

In Figures 13-1 and 13-2, the highest wave run-up ratio can be found at Probe#3, which reached the value of about three times of the incident wave amplitude in a period of 9 seconds. For Probe#6 and Probe#7 in a long wave period ($T > 12$ sec), large nonlinearity was found. For instance, at Probe#6 in a period of 12 seconds and the steepness of 1/16, the wave run-up which is 2.5 times of the incident wave was measured. Finally, considering the wave probes on the pontoon, Probe#4, Probe#5, Probe#6 and Probe#7, Probe#4 and Probe#5 do not have large nonlinearity compared to other wave probes on the pontoon. Thus, it is possible to consider that the highly nonlinear waves at Probe#6 and Probe#7 are a result of the effect of the columns.

3.4 Wave run-up – Summary

For both the head sea condition and the quartering sea condition, the performed ‘first order analysis’ is in good agreement with the linear potential solver except for the point where the wave escapes. Also, the wave probes located outside of the model showed better agreement. Moreover, as expected, the wave run-up ratio from the lower wave steepness has a better correspondence.

The maximum wave run-up ratio is observed at Probe#6 in the head sea condition. And the highest wave run-up ratio in a very long period ($T > 12$ sec) is found at Probe#6 in the quartering sea condition. In the head sea condition, the nearly trapped mode is found between two columns parallel to the wave direction. In the case of the quartering sea, the trapped mode is not easily defined. However, the columns and pontoons are assumed to cause the highly non-linear and random phenomenon at Probe#6 and Probe#7 in the quartering sea condition.



Fig. 8 Photo of the experiment: Heading 180°



Fig. 9 Photo of the experiment: Heading 225°

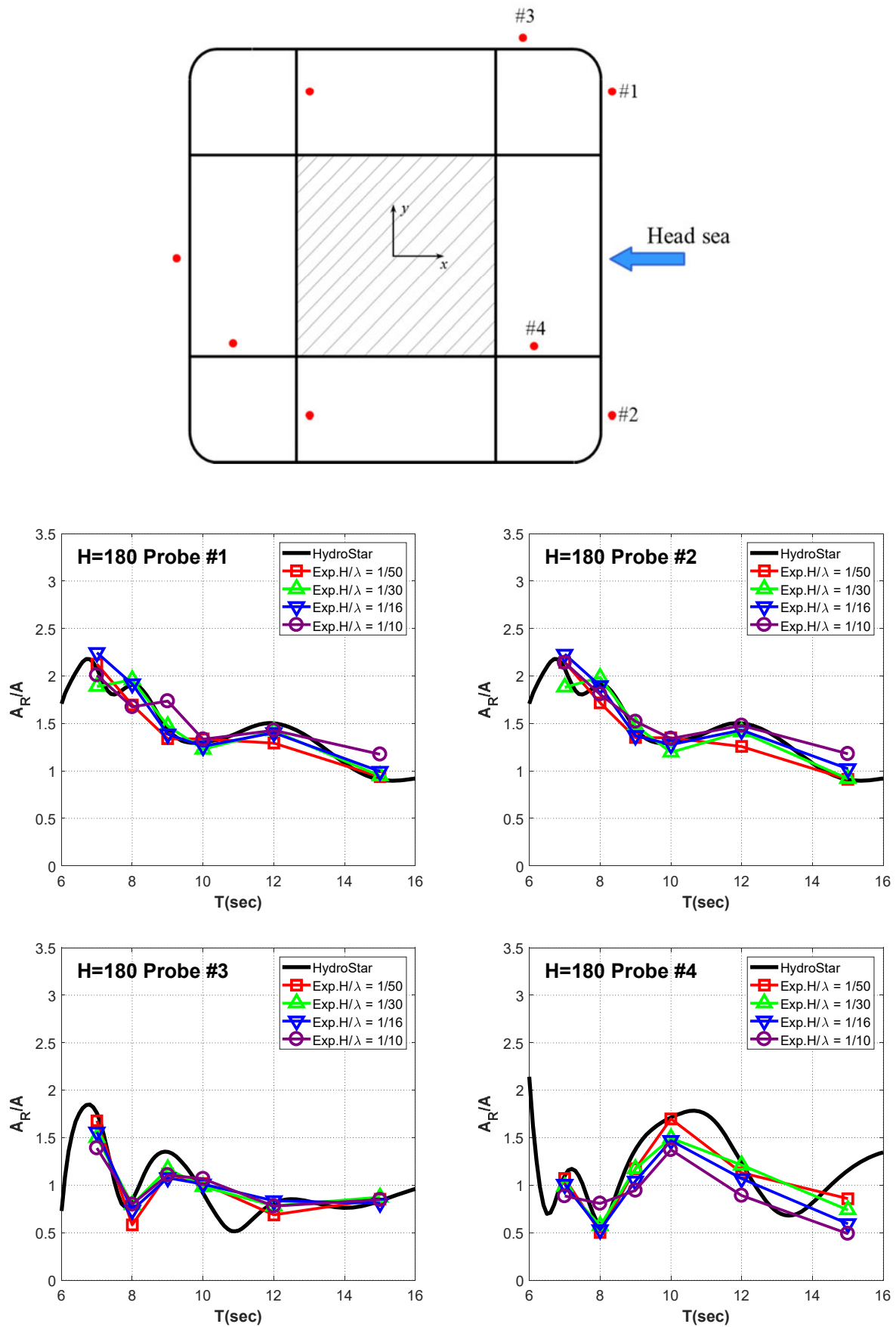


Fig. 10-1 Wave run-up ratio $H=180^\circ$ (first-order analysis)

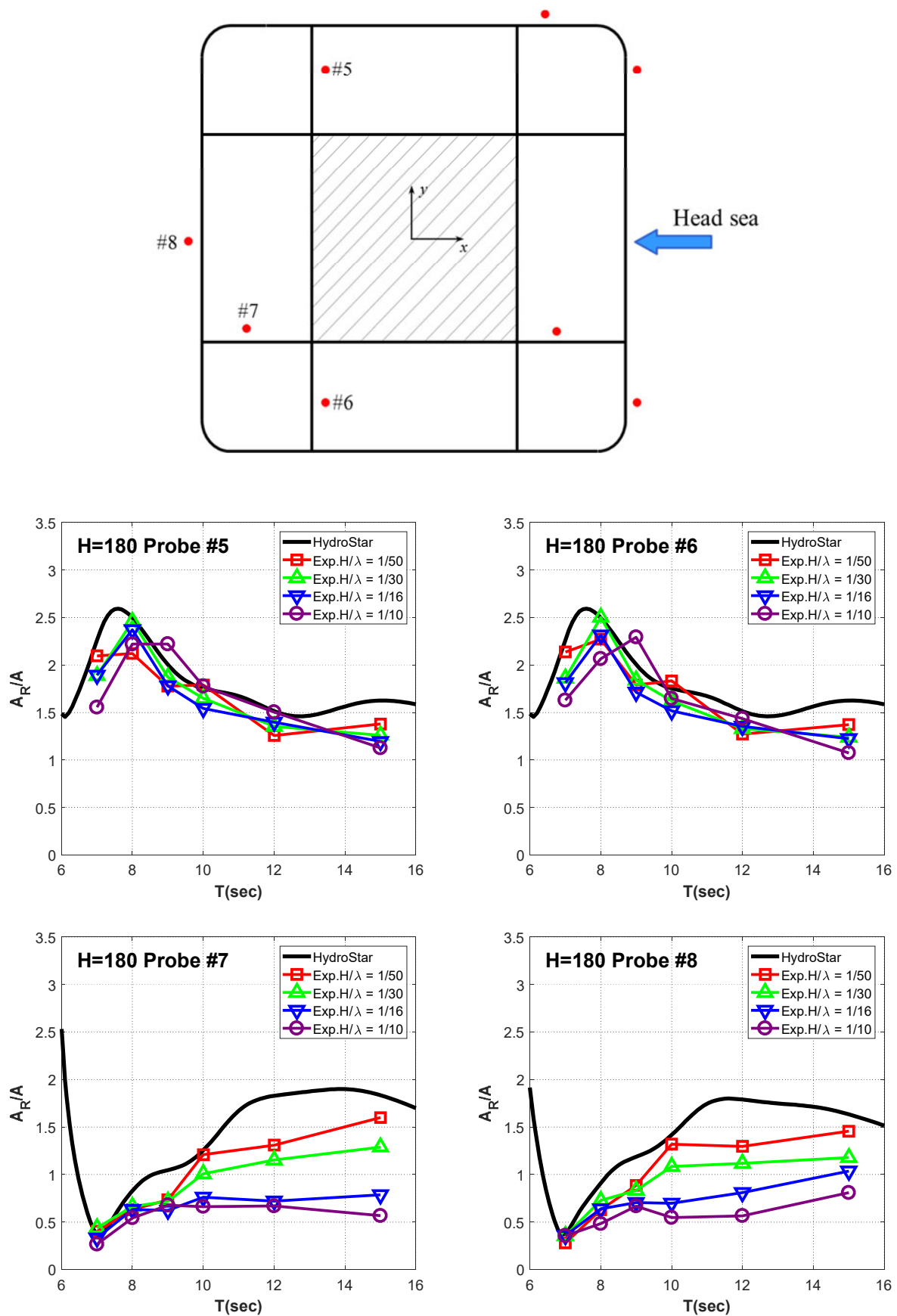


Fig. 10-2 Wave run-up ratio $H=180^\circ$ (first-order analysis)

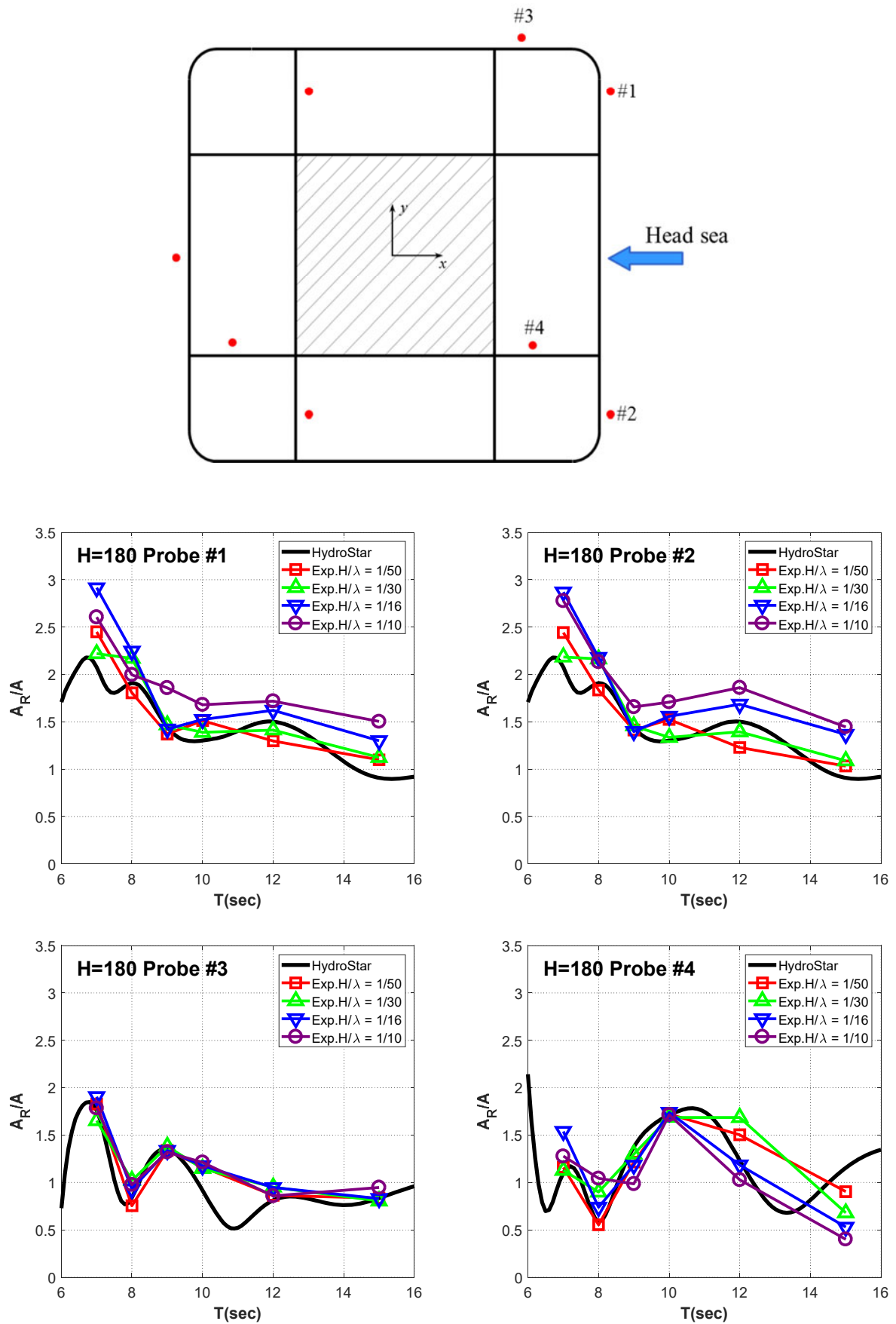


Fig. 11-1 Wave run-up ratio $H=180^\circ$ (full analysis)

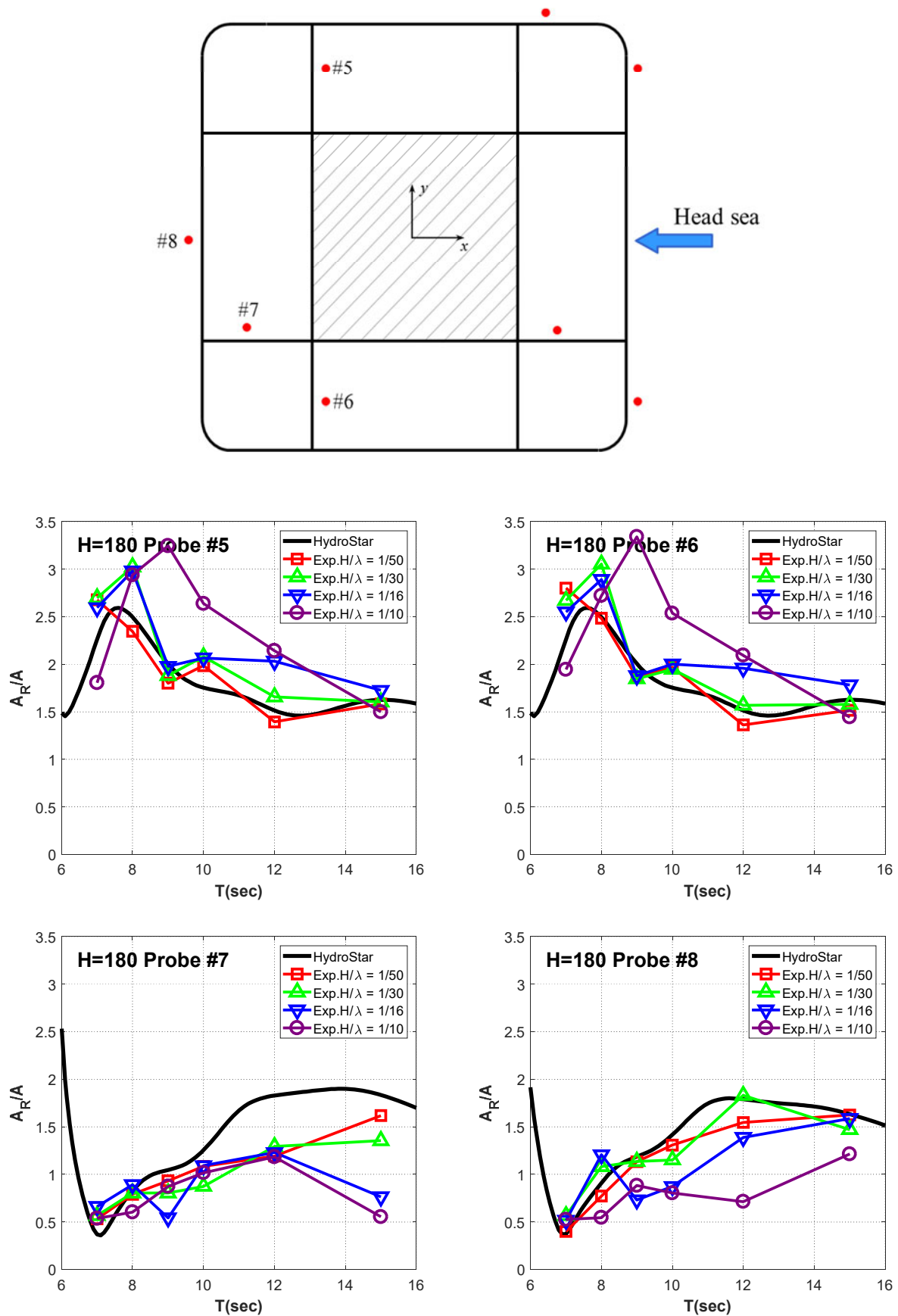


Fig. 11-2 Wave run-up ratio $H = 180^\circ$ (full analysis)

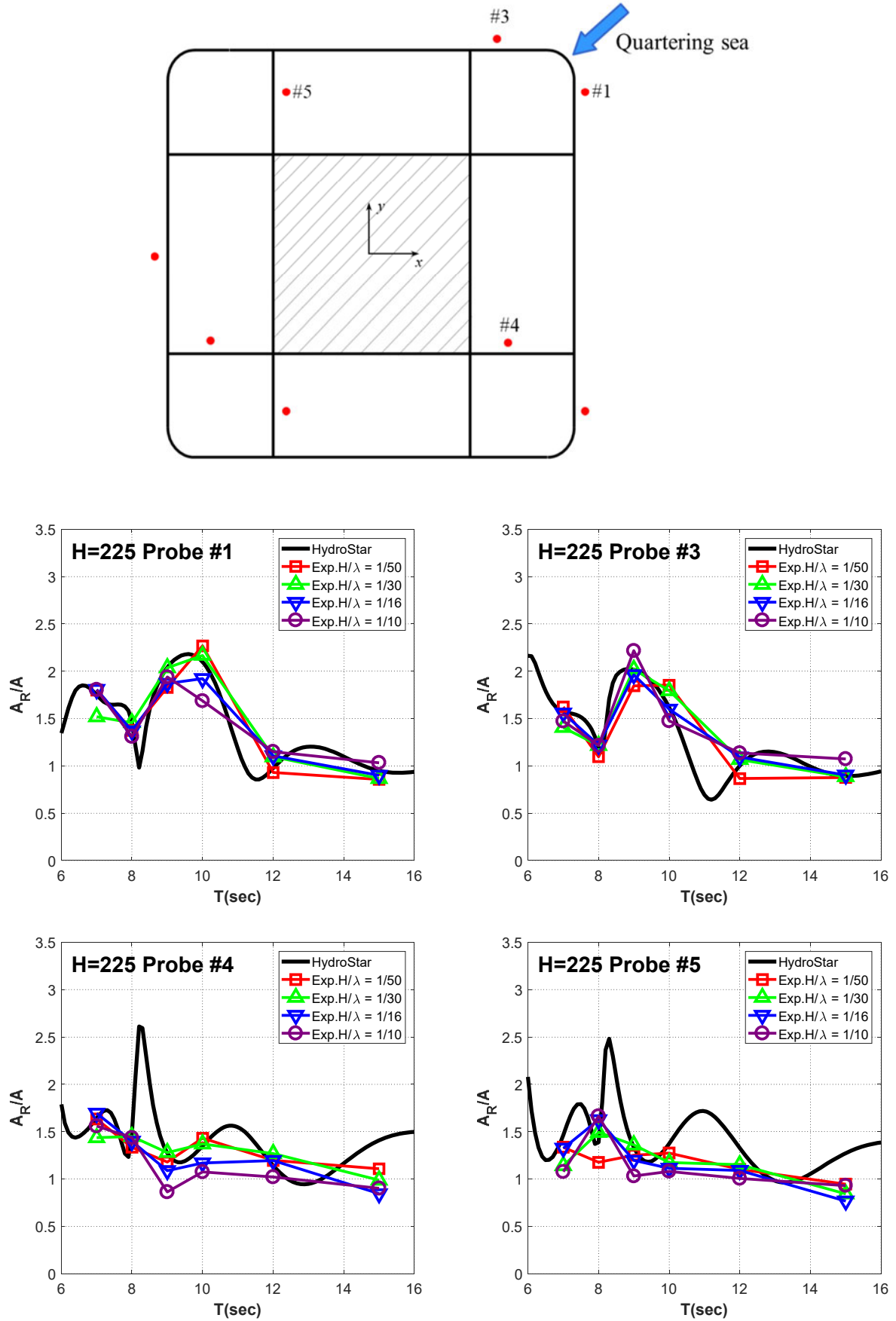


Fig. 12-1 Wave run-up ratio $H=225^\circ$ (first-order analysis)

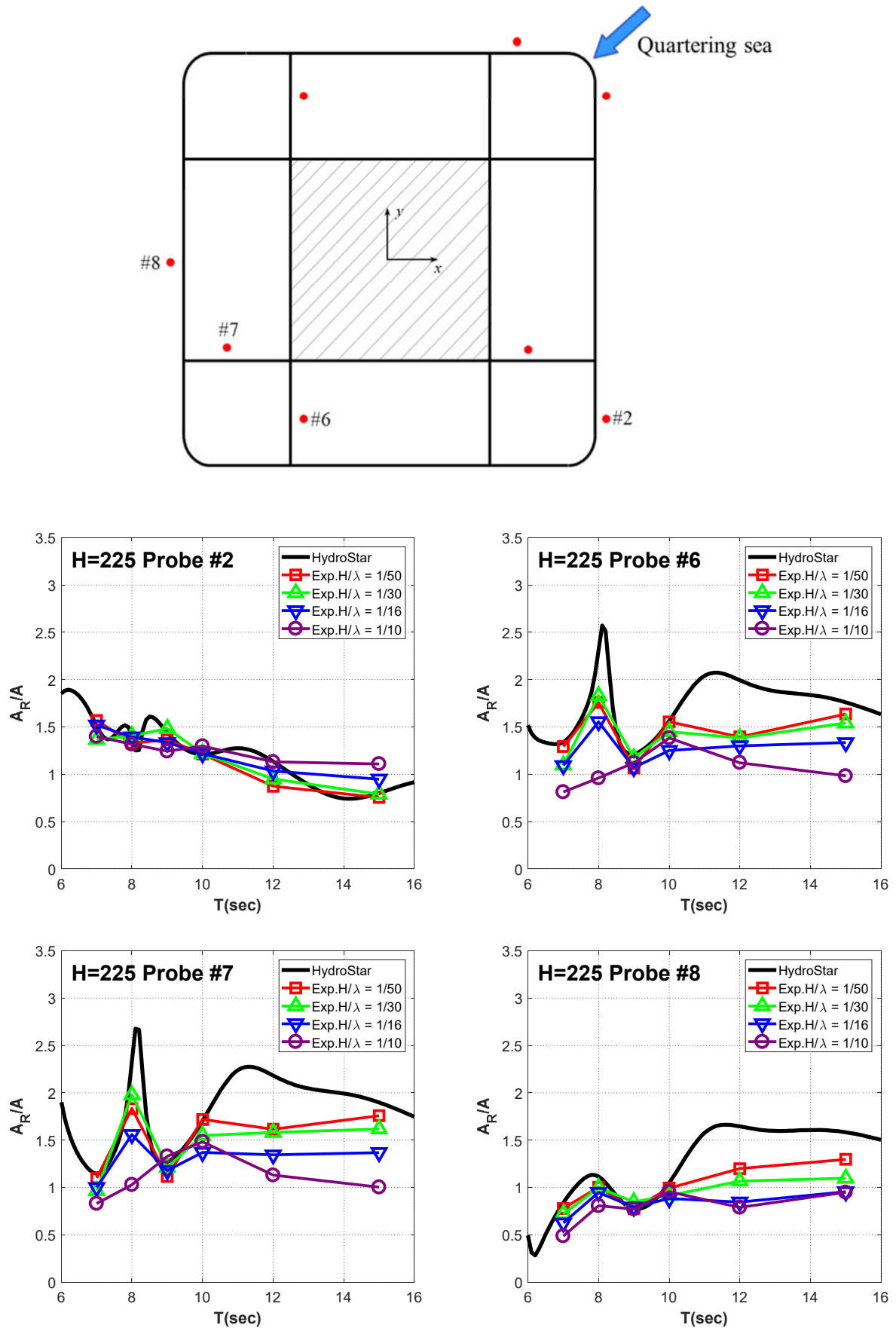


Fig. 12-2 Wave run-up ratio $H = 225^\circ$ (first-order analysis)

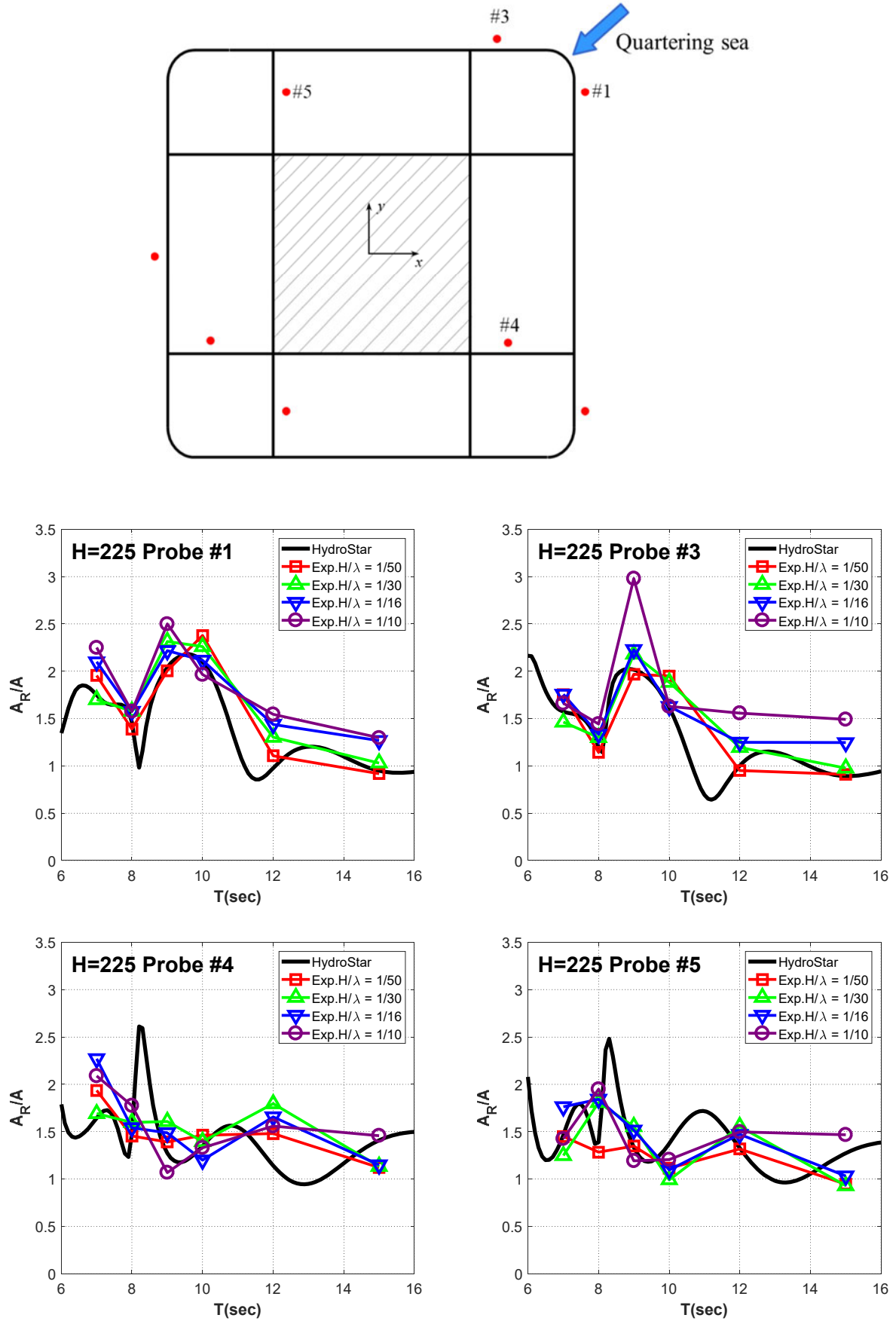


Fig. 13-1 Wave run-up ratio $H = 225^\circ$ (full analysis)

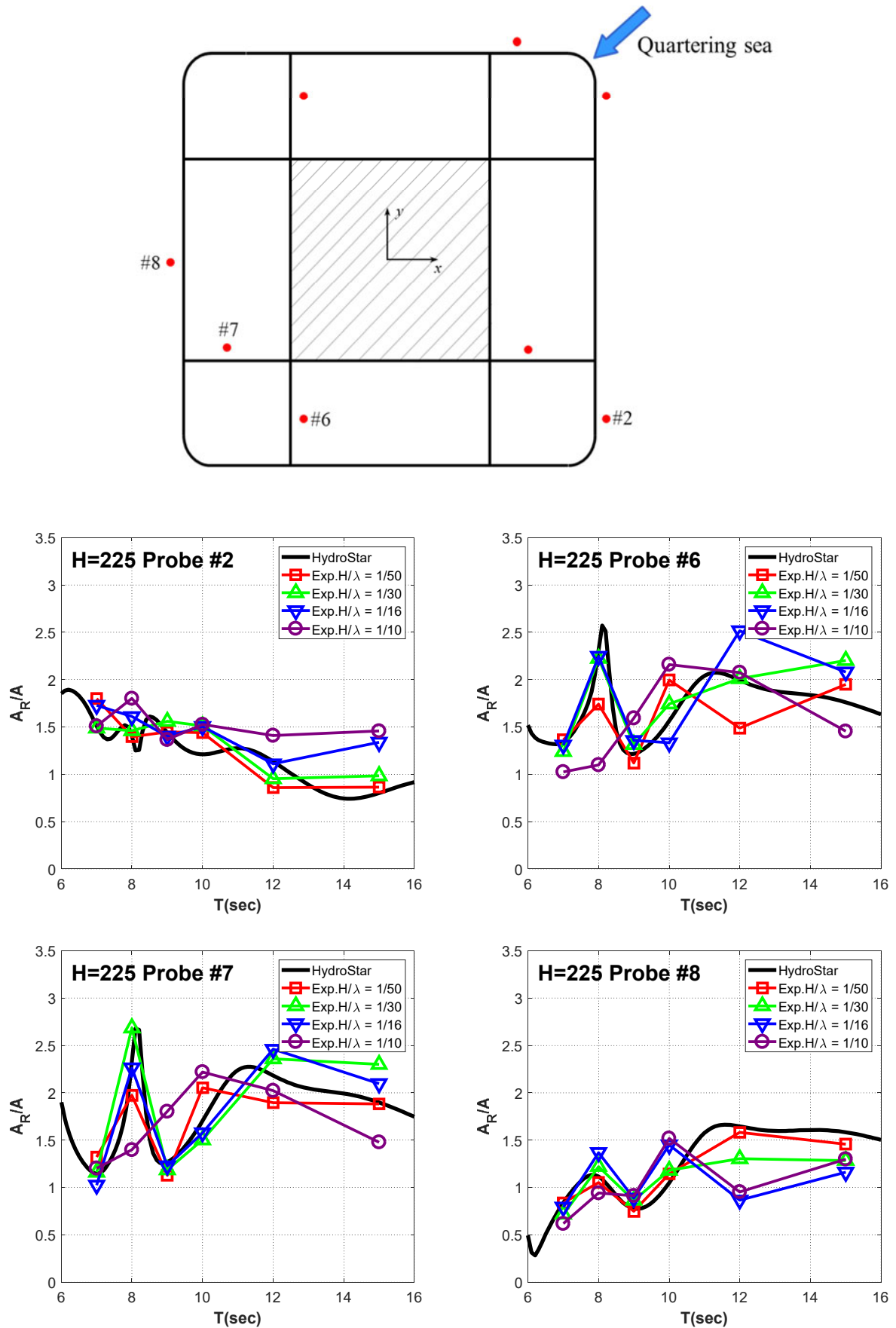


Fig. 13-2 Wave run-up ratio $H = 225^\circ$ (full analysis)

4. Conclusion

An experimental study was performed to calculate wave loads caused by wave run-up near a TLP platform. The purpose of the experiment was to develop fundamental technology for estimating the effects of marine environments on column-based offshore structures. Thus, no appendages were attached to the structure other than a pontoon. The experimental results confirmed that the wave run-up ratio varies according to changes in the incident angle and the incident wave period. An experiment on different wave steepnesses was also conducted to identify effects of non-linear wave phenomena.

The experimental results were compared with the results obtained from HydroStar, and the results confirmed that the overall tendency of the wave run-up could be identified by using a typical potential-flow based code. In particular, the potential-flow based code could effectively simulate the diffraction generated by the shape of the object. This was verified by the fact that a result similar to the resonance peak can be observed in both the potential solver calculations and the experimental result. However, some phenomena could not be estimated by using only the potential-flow based code. Under long wave period conditions, the wave run-up ratio at the point where the wave escapes was always underestimated in the experimental results compared to the HydroStar results.

The experimental results were derived from both the first-order analysis and the full analysis, and both results were compared to examine the size of the non-linear phenomena according to the periods and location. The non-linear phenomena were greater at the bow during a short wave period under both the head sea and the quartering sea conditions. Moreover, large-scale non-linear phenomena were generated between the front column and the rear column in a period of nearly 9 seconds under the head sea conditions, whereas these phenomena were observed at the rear column in a period of nearly 12 seconds under the quartering sea conditions.

Further experiments on the wave run-up at the floating platform will be performed to further develop the ultimate dynamic performance technology for estimating the effects of marine environments on column-based floating offshore structures. Therefore, a standard for estimating non-linear wave loads applied to practical platforms can be established by combining the results of this study with the results of further experiments.

ACKNOWLEDGMENT

This study was supported by a National Research Foundation of Korea (NRF) grant funded by the Korea government (MSIP) through GCRC-SOP (No. 2011-0030013) and supported by the Samsung Heavy Industry. Also, this research was supported by a grant from the Endowment Project of "Development of basis operation technique for running of the Deepsea Offshore Engineering Basin" funded by the Korea Research Institute of Ships and Ocean Engineering (PES9460).

REFERENCES

- [1] Eatock Taylor, R., & Sincok, P., 1989 Wave upwelling effects in TLP and Semi-submersible structure, *Ocean Engng.* 16, 281-306. [https://doi.org/10.1016/0029-8018\(89\)90021-8](https://doi.org/10.1016/0029-8018(89)90021-8)
- [2] J. M. NIEDZWECKI & J. R. HUSTON, 1992 Wave interaction with tension leg platforms, *Ocean Engng.* 19, 21-37. [https://doi.org/10.1016/0029-8018\(92\)90045-6](https://doi.org/10.1016/0029-8018(92)90045-6)
- [3] C.T. Stansberg, R. Baarholm, T. Kristiansen, E.W.M. Hansen, G. Rortveit, 2005 Extreme Wave Amplification and Impact Loads on Offshore Structures, OTC 17487. <https://doi.org/10.4043/17487-ms>
- [4] Bo Woo Nam, Namwoo Kim, Yonghwan Kim, Sa Young Hong and Hong Gun Sung, 2013 Computation of Nonlinear Wave Run-up around a Semi-submersible Platform, Proceedings of the PRADS2013, 809-815.

- [5] Fabio T. Matsumoto, Rafael A. Watai, Alexandre N. Simos, Marcos D. A. S. Ferreira, 2013 Wave Run-Up and Air Gap Prediction for a Large-Volume Semi-Submersible Platform, *J. Offshore Mech. Arct. Eng.* 135(1), 011302-011302-9. <https://doi.org/10.1115/1.4007380>
- [6] Seung Yoon Han, Sun Hong Kwon, Byeong Ju Kim, Young-Myung Choi, Jitae Do, Young Jun Yang, Sang Beom Lee, Dong Yeon Lee, 2014 Experimental and Numerical Study on Wave Run-Up, *Transactions of FAMENA*, 38(2), 11-20.
- [7] Bureau Veritas, 2016 HydroStar For Experts - User Manual, Version 6.3.
- [8] X.B. Chen, Hydrodynamics in Offshore and Naval Applications – Part I, 2004 Keynote lecture at the 6th Intl Conf HydroDynamics, (Perth)
- [9] J. Ramirez, P. Frigaard, T. Lykke Andersen, L. de Vos, 2013 Large scale model test investigation on wave run-up in irregular waves at slender piles, *Coastal Engineering* 72, 69-79. <https://doi.org/10.1016/j.coastaleng.2012.09.004>
- [10] B. Iwanowski, M. Lefranc, R. Wemmenhove, 2009 CFD Simulation of Wave Run-Up on a Semi-Submersible and Comparison With Experiment, *International Conference on Offshore Mechanics and Arctic Engineering*, 1, 19-29. <https://doi.org/10.1115/omae2009-79052>
- [11] L.F. Chen, J. Zang, A.J. Hillis, G.C.J. Morgan, A.R. Plummer, 2014 Numerical investigation of wave-structure interaction using OpenFOAM, *Ocean Engineering*, 88, 91–109. <https://doi.org/10.1016/j.oceaneng.2014.06.003>
- [12] H. Cao, J. Zha, D. Wan, 2011 Numerical Simulation of Wave Run-up around a Vertical Cylinder, *Proceedings of the International Offshore and Polar Engineering Conference*, 1 726-733.
- [13] N. Abdussameia, R. Ojeda, Y. Drobyshevskib, G. Thomasc, W. Amina, 2016 Experimental investigation of extreme wave impacts on a rigid TLP model in cyclonic conditions, *Ships and Offshore Structures*, 13, 153-170. <https://doi.org/10.1080/17445302.2015.1121608>

Submitted: 22.01.2018

Accepted: 12.10.2018

Dong Woo Jung
Korea Research Institute of Ships &
Ocean Engineering, Daejeon, South Korea
Young Jun Kim
Young Jun Yang
Sun Hong Kwon
Department of Naval Architecture and
Ocean Engineering, Pusan National
University, Busan, South Korea